An International Journal of Optimization and Control: Theories & Applications
ISSN: 2146-0957 eISSN: 2146-5703
Vol.x, No.x, pp.xx-xx (2026)
https://doi.org/10.36922/IJOCTA026310196

RESEARCH ARTICLE

Hybridization of the weighted distance method with directional bat algorithm for NMPC tuning

Misael Hernández[1], Luis Miguel Valenzuela[1*], Antioco López-Molina[1], Carolina Conde-Mejía[1], Fernando Israel Gómez-Castro[2], Oscar Daniel Lara-Montaño[3], and Moisés Abraham Petriz-Prieto[1]

[1]División Académica Multidisciplinaria de Jalpa de Méndez, UJAT, Carretera Nacajuca–Jalpa de Méndez, R/a Rivera Alta, Jalpa de Méndez, Tabasco, México
[2]División de Ciencias Naturales y Exactas, Departamento de Ingeniería Química, Universidad de Guanajuato, Campus Guanajuato, Noria Alta S/N Col. Noria Alta, Guanajuato, México
[3]Facultad de Ingeniería, Campus Amealco, Universidad Autónoma de Querétaro, Carretera Amealco–Atemascalcingo Km 1, Centro, Amealco de Bonfil, Querétaro, México
aguilamisahdz97@gmail.com, luismy1983emanuel@gmail.com, antioco.lopez@ujat.mx, carolina.conde@ujat.mx, fgomez@ugto.mx, oscar.lara@uaq.mx, iqmapp@gmail.com

ARTICLE INFO

Article history:
Received: August 1, 2026
Revised: October 16, 2026
Accepted: October 20, 2026
Published Online: November 3, 2026

Keywords:
Directional bat algorithm
Weighted distance method
Optimization
Metaheuristic
Predictive control

AMS Classification 2010:
90C59; 90C26; 93C95

ABSTRACT

This work presents a hybrid optimization algorithm that combines the Weighted Distance Method and the Directional Bat Algorithm to improve the efficiency and robustness of solving nonlinear model predictive control problems. The proposed hybrid framework integrates the global exploration capability of the Directional Bat Algorithm with the local exploitation and adaptive refinement properties of the Weighted Distance Method. In the first stage, the Directional Bat Algorithm generates a diverse set of candidate solutions by using adaptive mechanisms for frequency, amplitude, and random movement, thereby ensuring broad coverage of the search space and preventing premature convergence to local minima. Subsequently, the Weighted Distance Method refines these solutions by computing weighted directional vectors, which are updated at each iteration based on the population mean distance and each agent's proximity to the global best individual. The sequential combination of both strategies achieves an effective balance between exploration and exploitation, resulting in greater stability, improved convergence performance, and higher-quality optimal solutions. On a standard suite of thirty benchmark functions in dimensions 10, 30, and 50, the hybrid ranks third among five optimizers: it outperforms both of its constituent algorithms but does not surpass the Differential Evolution and Particle Swarm baselines, confirming that the sequential coupling yields a stronger optimizer than either component alone. On the tuning of a nonlinear model predictive controller for a Van de Vusse reactor, the proposed hybrid scheme achieves competitive closed-loop tracking performance compared with the standalone methods while improving convergence stability and robustness to initialization, highlighting its potential for complex nonlinear control applications.

CC BY

1. Introduction

Industrial process systems, including chemical reactors, energy systems, and multivariable plants, frequently exhibit nonlinear dynamics, interacting inputs and outputs, and operating constraints. These characteristics can limit the effectiveness of conventional linear control strategies and motivate the use of advanced model-based approaches. Model predictive control (MPC) has become an established technology in process industries because it explicitly accounts for process dynamics

*Corresponding Author

and constraints through repeated finite-horizon optimization.[1–3] Nonlinear model predictive control (NMPC) extends this framework to systems for which nonlinear models are needed to represent the process behavior more faithfully.[4–6] Its practical performance, however, depends not only on the prediction model and horizon lengths but also on the choice of the objective-function weights that balance tracking errors, control effort, and, in some formulations, multiple performance objectives.

The selection of NMPC tuning parameters is therefore a nontrivial optimization task. Vallerio *et al.*[7] addressed this issue through a multi-objective optimization procedure, emphasizing the competing nature of tracking, disturbance rejection, and control effort, and showing how Pareto solutions can inform the choice of weights. Flores-Tlacuahuac *et al.*[8] likewise studied multi-objective NMPC for chemical reactors, illustrating the relevance of explicitly considering competing control objectives in nonlinear process applications. More recently, Giraldo *et al.*[9] proposed a hybrid tuning procedure combining goal-attainment optimization with variable-neighborhood search to determine objective-function weights and controller horizons. Comprehensive surveys, such as those by Al Bannoud *et al.*[10] and Ölmez *et al.*,[11] highlight the growing reliance on systematic optimization for control parameter tuning across chemical processes and control systems. Together, these studies demonstrate that controller tuning can be formulated systematically rather than relying exclusively on manual or trial-and-error adjustment.[12] They also show that tuning frameworks may differ in their decision variables, objective formulations, and treatment of computational cost.

Metaheuristic optimization is attractive for such tuning problems because the closed-loop performance function may be nonlinear, nonconvex, expensive to evaluate, and unavailable in a convenient, differentiable form. Population-based methods such as particle swarm optimization (PSO), differential evolution (DE), and the bat algorithm (BA) provide derivative-free search mechanisms.[13–16] Reviews and comparative studies have surveyed the breadth of metaheuristic methods and their engineering applications,[9,15,17–20] while also highlighting that their performance is problem-dependent and that global optimality is generally not guaranteed.[17,18] The No Free Lunch theorems further caution against assuming that a single optimizer will dominate across all problem classes.[21] Accordingly, algorithmic comparisons should use transparent experimental protocols and relevant baselines, rather than relying on claims of universal superiority.

Recent NMPC and process control studies illustrate several ways in which optimization and learning strategies are being integrated into controller design and implementation. Kusznir and Smoczek[22] combined an evolutionary data-driven prediction model with PSO-based NMPC for an overhead crane, while Devanathan *et al.*[23] investigated an NMPC framework for Internet of Things applications using enhanced PSO and cloud computing. Optimization-based control has also been successfully applied across diverse practical systems, including longitudinal flight control,[24] autonomous mowers,[25] microgrid load frequency control,[26] and industrial SCR units.[27] Furthermore, data-driven frameworks, Koopman operator techniques, and Bayesian approaches have been explored for predictive control auto-tuning and modeling.[28–31] For the Van de Vusse reactor specifically, Ankalugari *et al.*[32] explored deep reinforcement learning as an alternative control approach. While these contributions broaden the application landscape, they address different design questions, including online optimization architecture, surrogate modeling, or alternative control paradigms, and do not, by themselves, resolve the specific issue considered here: how to tune NMPC penalty weights using a hybrid population-based optimizer that combines complementary search operators.

Hybrid metaheuristics have been developed to coordinate complementary search behaviors and mitigate limitations associated with using a single search operator. For example, Wang *et al.*[33] coupled multiple strategies within a bat algorithm, while Yu *et al.*[34] proposed an adaptive multistage structure for BA to address premature convergence. Other hybrid frameworks integrate mechanisms such as Lévy flights, quantum-inspired operations, or population diversification to enhance search efficiency.[35–38] More generally, hybrid and adaptive methods seek to maintain an effective balance between exploration (searching broadly across the feasible domain) and exploitation (refining candidate solutions in promising regions).[9,15,17,39] However, the design of a hybrid should be justified by its algorithmic structure and empirical evidence. Wang *et al.*[3] specifically urge greater scrutiny of novelty claims in metaheuristic research, reinforcing the need to distinguish a genuinely evaluated mechanism from a new metaphor or an untested combination. Thus,

the relevant research question is not whether hybridization is inherently superior, but whether a particular coupling produces measurable benefits under controlled comparisons.

In this work, we investigate a sequential hybridization of the Directional Bat Algorithm (dBA)[40] and the Weighted Distance Method (WDM). The dBA stage generates candidate displacements using its directional bat-search mechanism, whereas WDM updates candidates through adaptive weights derived from distance information and the current best solution. The hybrid applies both operators to the same population during each generation, with the aim of combining population-level diversification and distance-guided refinement. The study focuses specifically on the offline tuning of the diagonal weighting matrices of an NMPC controller for the Van de Vusse reactor. This reactor has a long history as a challenging nonlinear control benchmark because of its nonlinear reaction kinetics and controllability characteristics.[41,42] Existing NMPC tuning studies[7,8,10] and recent optimization-based control applications[22,23,29] provide the broader context; nevertheless, within the literature reviewed for this study, we did not identify a systematic evaluation of this particular WDM–dBA coupling for NMPC weight tuning, including matched-budget benchmark comparisons and an ablation of the coupling strategy. This is a scoped research gap, rather than a claim that no related hybrid optimizer or distance-based method exists.

To examine the proposed approach without presuming that hybridization guarantees an improvement, we evaluate WDM-dBA against its two constituent algorithms and the PSO and DE baselines. The evaluation includes standardized benchmark functions, paired independent runs, statistical comparisons, and an ablation of alternative coupling schedules. The resulting optimizer is then applied to the NMPC tuning problem for the Van de Vusse reactor, where closed-loop tracking, control actions, convergence behavior, and sensitivity to initialization are considered. The paper's contributions are summarized as follows:

(a) Development of WDM.We formulate a distance-based population optimizer in which normalized adaptive weights and population-distance information determine candidate displacements.
(b) Development and evaluation of the sequential WDM-dBA hybrid. We couple dBA and WDM within each generation and assess the hybrid against both component algorithms and established PSO and DE baselines under a matched evaluation budget.
(c) Statistical benchmark and coupling-ablation study. We evaluate the methods on the CEC 2014 benchmark suite at multiple dimensions using paired runs and statistical tests and examine whether operator order and coupling schedule affect performance.
(d) Application to NMPC weight tuning. We use the proposed hybrid to tune the diagonal penalty matrices of an NMPC controller for the Van de Vusse reactor and assess closed-loop tracking and manipulated-variable behavior.
(e) Analysis of computational effort and robustness. We compare convergence behavior and computational cost and examine variability across initializations, while interpreting any observed benefit in light of the study's benchmark and single-process scope.

2. Model predictive control

MPC is an advanced control strategy in which a constrained optimization problem is solved at each sampling instant. Since its development in the 1970s, MPC has become a well-established and widely adopted approach for the stabilization and control of nonlinear dynamical systems in the presence of uncertainties and time delays, particularly in process control applications. This methodology relies on an explicit model of the system to predict its future behavior over a finite prediction horizon. Based on these predictions, an optimal sequence of control actions is determined by minimizing a predefined cost function, subject to system constraints.[3]

The cost function typically penalizes both the deviation of state variables from their reference trajectories and the control effort, while explicitly accounting for constraints on state variables and control inputs. Although the optimization yields an optimal sequence of control actions over the entire prediction horizon, only the first control action is implemented.

At the subsequent sampling instant, the prediction horizon is shifted forward, and the optimization problem is solved again using updated system measurements. This iterative procedure, commonly referred to as the receding horizon strategy, enables continuous updating of model predictions and compensation for disturbances and uncertainties, thereby enhancing the performance and robustness of the control system.

Therefore, the following cost function is defined:

$$\begin{aligned}\mathbf{J} = &\sum_{i=1}^{n_y}\sum_{n=1}^{N_p} Q_{ii}[\hat{y}_i(k+n \mid k) - r_i(k+n)]^2 \\ &+ \sum_{j=1}^{n_u}\sum_{n=1}^{m_j} W_{jj}[\Delta u_j(k+n-1)]^2\end{aligned} \tag{1}$$

subject to the following constraints:

$$\begin{aligned}
\mathbf{x}(k+n) &= f(k, \mathbf{x}(k+n-1), \mathbf{u}(k+n-1), \boldsymbol{\rho}), \\
0 &= g(\hat{\mathbf{y}}(k+n), \mathbf{x}(k+n), \mathbf{u}(k+n), \boldsymbol{\rho}), \\
n &= 1, ..., N_p \\
\mathbf{x}(k) &= \hat{\mathbf{x}}(k), \\
\Delta u_{j,\min} &\leq u_j(k+n-1) - u_j(k+n-2) \\
&\leq \Delta u_{j,\max}, \\
j &= 1, ..., n_u, \ n = 1, ..., m_j \\
y_{i,\min} &\leq \hat{y}_i(k+n) \leq y_{i,\max}, \\
i &= 1, ..., n_y,
\end{aligned}$$

where $\mathbf{u}$ denotes the vector of manipulated (input) variables, $\mathbf{y}$ represents the vector of measured outputs, and $\mathbf{x}$ is the state vector; $\boldsymbol{\rho}$ denotes the vector of disturbance parameters. The numbers of controlled outputs and manipulated inputs are denoted by n_y and n_u, respectively. The prediction horizon is given by N_p, while m_j is the control horizon associated with the j-th input. The matrices $\mathbf{Q}$ and $\mathbf{W}$ correspond to the output error weighting matrix and the control increment weighting matrix, respectively.

The predicted value of the i-th controlled output at step n of the prediction horizon is denoted by $\hat{y}_i(k+n \mid k)$, where k represents the current sampling instant. An appropriate selection or tuning of the penalty parameters is essential to avoid undesirable oscillations in the controlled variables.

3. WDM algorithm

Metaheuristic algorithms commonly approximate solutions to optimization problems by employing a population of candidate solutions, which are iteratively refined through information exchange mechanisms and algorithm-specific parameters.

In this work, a new optimization algorithm, termed WDM, is introduced. This metaheuristic approach guides the search process by iteratively updating a set of candidate solutions within the search space. The movement of each solution is governed by three fundamental components: (i) the distance between the solution and a reference point, (ii) a unit vector that defines the direction of motion, and (iii) an adaptive weighting mechanism that regulates the step size of each agent.

The objective function constitutes a core component of the control-oriented optimization framework. Its main purpose is to ensure that the predicted system output over the prediction horizon closely follows a desired reference trajectory, while simultaneously penalizing both the tracking error and the control effort, as defined in **Equation (1)**. In this study, the associated penalty parameters are tuned using the proposed WDM algorithm, which optimizes them through an information exchange process among stochastic agents. This approach enables the design of control strategies that yield smooth and robust dynamic responses in the presence of disturbances and process uncertainties.

3.1. Problem formulation and initialization

The proposed method is designed to address continuous optimization problems without relying on gradient information, and can be formulated as follows:

$$\min_{\mathbf{x}\in\Omega} f(\mathbf{x}), \quad \Omega = [\mathbf{L_b}, \mathbf{U_b}] \subset \mathbb{R}^d \tag{2}$$

where $f : \mathbb{R}^d \to \mathbb{R}$ denotes the objective function, d is the dimensionality of the search space, and $\mathbf{L_b}, \mathbf{U_b} \in \mathbb{R}^d$ represent the lower and upper bounds of the feasible domain, respectively.

The initialization phase consists of generating a population of n random agents within the search domain, along with defining the maximum number of iterations $t_{\max}$, as given by:

$$\mathbf{x}_i^{(0)} = \mathbf{L_b} + (\mathbf{U_b} - \mathbf{L_b}) \cdot \mathbf{r}_i, \quad i = 1, \ldots, n \tag{3}$$

where $\mathbf{r}_i \sim U(0,1)^d$ denotes a $d \times 1$ vector of uniformly distributed random variables. For each agent, a historical position $\mathbf{x}_i^{\text{old}}$ is defined, which is initially set equal to $\mathbf{x}_i^{(0)}$. The initial objective function value is assigned as $f_i^{(0)} = +\infty$ to ensure the acceptance of the first valid update. The best initial individual is then selected arbitrarily from the population.

3.2. Main loop (iterations up to t_{max})

The average population distance is computed at each iteration t based on the distance between each agent and the current global best solution. For each agent i, this distance defined as follows:

$$\delta_i^{(t)} = \left\| \mathbf{x}^\star(t) - \mathbf{x}_i^{(t)} \right\|_1 = \sum_{j=1}^{d} \left| x_{i,j}^\star(t) - x_{i,j}^{(t)} \right|. \quad (4)$$

The average population distance is then computed from these distances:

$$d_m^{(t)} = \frac{1}{n} \sum_{i=1}^{n} \delta_i^{(t)} \quad (5)$$

which adaptively regulates the magnitude of the displacements.

Within the main iteration loop at step t, an inner loop is executed to iterate over the population of agents, $i = 1, \ldots, n$.

To maintain population diversity, each agent generates a random reference point within the search domain:

$$\mathbf{P}_i^{(t)} = \mathbf{L_b} + (\mathbf{U_b} - \mathbf{L_b}) \cdot \mathbf{r}_i. \quad (6)$$

The scanning direction is defined as a vector normalized with respect to the ℓ_1 norm:

$$\mathbf{v}_i^{(t)} = \frac{\mathbf{P}_i^{(t)} - \mathbf{x}_i^{(t)}}{\|\mathbf{P}_i^{(t)} - \mathbf{x}_i^{(t)}\|_1}. \quad (7)$$

3.3. Adaptive weighting mechanism

The magnitude of each agent's displacement is regulated by an adaptive weighting vector $\mathbf{w}_{i,j}^{(t)}$, defined according to the agent's role within the population.

(1) For the global best individual, $i = I$, an explicit mechanism is introduced to promote exploration:

$$\mathrm{comp}_{i,j}^{(t)} = \frac{1}{\left| \mathbf{x}_{i,j}^{(t)} - \mathbf{x}_{i,j}^{\mathrm{old}} \right|}. \quad (8)$$

Equation (8) indicates that smaller components lead to larger weights, thereby facilitating escape from stagnation. In cases where any denominator becomes zero, the distances to other randomly selected agents are used instead.

$$\mathrm{comp}_{i,j}^{(t)} = \frac{1}{\left| \mathbf{x}_{i,j}^{(t)} - \mathbf{x}_{k,j} \right|}. \quad (9)$$

If the problem persists, the domain size is used:

$$\mathrm{comp}_{i,j}^{(t)} = \frac{1}{|\mathbf{U_b} - \mathbf{L_b}|}. \quad (10)$$

Finally, the components are normalized:

$$\mathbf{w}_{i,j}^{(t)} = \frac{\mathrm{comp}_{i,j}^{(t)}}{\max_k \left(\mathrm{comp}_{i,k}^{(t)} \right)}. \quad (11)$$

(2) For non-optimal agents $i \neq I$,

$$comp_j = \left| \mathbf{x}_j^* - \mathbf{x}_{i,j} \right|, \quad (12)$$

Equation (12) induces attraction toward the global best solution.
If a random agent coincides with the global best, a correction is applied as in Case 1, followed by normalization:

$$\mathbf{w}_{i,j}^{(t)} = \frac{\mathrm{comp}_{i,j}^{(t)}}{\max_k \left(\mathrm{comp}_{i,k}^{(t)} \right)}. \quad (13)$$

This mechanism enables a balance between the exploration and exploitation phases of the algorithm.

3.4. Solution update, selection criteria, and global best update

The candidate position of each agent is updated as follows:

$$\mathbf{x}_i^{(t+1)} = \mathbf{x}_i^{(t)} + \mathbf{w}_{i,j}^{(t)} d_m^{(t)} \mathbf{v}_i^{(t)}. \quad (14)$$

The adaptive weighting mechanism guarantees that the total displacement remains bounded by $d_m^{(t)}$.

Proposition 1 (Bounded adaptive displacement)**.** *Let*

$$\mathbf{w}_{i,j}^{(t)} = \frac{\mathrm{comp}_{i,j}^{(t)}}{\max_k \mathrm{comp}_{i,k}^{(t)}}, \ \textit{for } j = 1, \ldots, d.$$

If

$$\boldsymbol{\Delta} x_i^{(t)} = \mathbf{w}_{i,j}^{(t)} d_m^{(t)} \mathbf{v}_i^{(t)},$$

then

$$\boxed{\left\| \boldsymbol{\Delta} x_i^{(t)} \right\|_1 \leq d_m^{(t)}.}$$

Consequently, the adaptive weighting mechanism regulates the individual contribution of each decision variable to the update in (14)*. By scaling the direction vector* $\mathbf{v}_i^{(t)}$ *via* $\mathbf{w}_{i,j}^{(t)}$*, the total displacement is redistributed among the dimensions while preserving* $d_m^{(t)}$ *as an absolute upper bound on its* ℓ_1*-norm.*

Proof. From (8), (9) and (10) it follows that $\text{comp}_{i,j}^{(t)} > 0$. Since $\text{comp}_{j}^{(t)} < \max_k \text{comp}_{i,k}^{(t)}$, normalization yields

$$0 < \mathbf{w}_{i,j}^{(t)} = \frac{\text{comp}_{i,j}^{(t)}}{\max_k \text{comp}_{i,k}^{(t)}} \leq 1.$$

By the hypothesis,

$$\boldsymbol{\Delta} x_i^{(t)} = \mathbf{w}_{i,j}^{(t)} d_m^{(t)} \mathbf{v}_i^{(t)},$$

we have that

$$\begin{aligned} \|\boldsymbol{\Delta} x_i^{(t)}\|_1 &= d_m^{(t)} \sum_{j=1}^{d} \mathbf{w}_{i,j}^{(t)} |\mathbf{v}_{i,j}^{(t)}| \\ &\leq d_m^{(t)} \sum_{j=1}^{d} |\mathbf{v}_{i,j}^{(t)}| \\ &= d_m^{(t)} \|\mathbf{v}_i^{(t)}\|_1 = d_m^{(t)}. \end{aligned}$$

Hence,

$$\|\boldsymbol{\Delta} x_i^{(t)}\|_1 \leq d_m^{(t)}.$$

□

Subsequently, a projection operator is applied to ensure that the solutions remain within the feasible domain:

$$x_{ij}^{(t+1)} = \min\left(\max(x_{ij}^{(t+1)}, L_{b,j}), U_{b,j}\right). \quad (15)$$

At each iteration of the while loop, if any candidate solution attains a better objective value than its current value, the corresponding agent position is updated; that is, if

$$f\left(\mathbf{x}_i^{(t+1)}\right) < f\left(\mathbf{x}_i^{(t)}\right), \quad (16)$$

the candidate position is accepted, and the global best individual is defined as follows:

$$\mathbf{x}^\star = \arg\min_i f(\mathbf{x}_i), \quad f^\star = \min_i f(\mathbf{x}_i). \quad (17)$$

The evolution of the best objective value is recorded to enable convergence analysis. The algorithm proceeds until the maximum number of iterations, $t_{\max}$, is reached. Upon termination, the best solution found and its corresponding objective function value are returned.

The updated best objective is subsequently stored in the convergence curve $Conv_f$, allowing continuous monitoring of the algorithm's performance throughout the optimization process.

4. WDM hybridization with dBA

The proposed hybrid WDM-dBA algorithm combines the exploratory capabilities of dBA with the local refinement and adaptive adjustment features of WDM. This integration is intended to exploit the complementary strengths of global exploration and local exploitation, thereby enhancing both the efficiency and robustness of the optimization process.

In particular, the proposed framework is designed to improve search performance in complex optimization problems arising in NMPC, where nonconvexity and high dimensionality often hinder convergence toward the global optimum.

4.1. dBA phase: Global exploration

The first phase of the hybrid algorithm is based on dBA, introduced in,[40] which plays a key role in the global exploration of the search space. Its primary objective is to identify promising regions through a controlled stochastic search, thereby reducing the likelihood of premature convergence to local minima. During this phase, the population dynamics are governed by mechanisms inspired by the echolocation behavior of bats, where each agent updates its position and velocity according to its frequency, loudness, and pulse emission rate.

This exploration stage provides a robust initialization for the subsequent exploitation phase, ensuring broad coverage of the search domain while maintaining population diversity.

In the first stage, corresponding to dBA, a global exploration of the search space is carried out as follows:

(a) An initial population of candidate solutions is generated within the predefined bounds $[L_b, U_b]$.
(b) Each bat represents a candidate solution vector x_i in the search space.
(c) The frequencies, positions, and loudness parameters are updated according to adaptive control parameters A and r, which evolve throughout the iterations (typically decreasing and increasing, respectively).
(d) Stochastic movements, governed by the factors f_1 and f_2, together with guidance from the current global best solution, promote an effective and diversified exploration of the search domain.

This stage acts as a global diversification mechanism, reducing the risk of premature convergence and enhancing the identification of promising regions within the search space.

4.2. WDM phase: local operation

The second phase of the hybrid scheme corresponds to WDM, whose objective is to intensify the search within the promising regions previously identified by dBA. In this stage, the algorithm emphasizes the refinement of candidate solutions through a local adjustment process guided by structural information derived from the population.

In contrast to the preceding phase, where global diversification predominates, WDM focuses on exploiting the search space by progressively improving solutions located in the vicinity of high-quality candidates. This is achieved by leveraging spatial relationships and proximity measures among individuals, enabling a more directed and efficient search process. Consequently, the method promotes more accurate and stable convergence, enhancing the quality of the obtained solutions.

Building upon the candidate solutions generated during the dBA phase, WDM is subsequently applied to intensify the search within the most promising regions:

(a) The method computes weighted directional vectors based on the average distances among individuals in the population.
(b) Each agent updates its position using a normalized weighted direction vector that balances the influence of neighboring solutions.
(c) Candidate solutions are iteratively refined toward more promising regions through an adaptive weighting mechanism.

This procedure promotes an adaptive directional search, enhancing local convergence toward high-quality solutions.

4.2.1. Hybrid WDM-dBA integration

The integration phase constitutes the core of the proposed WDM-dBA scheme, as it defines how global exploration and local exploitation strategies are coordinated within the optimization process. The primary objective of this stage is to achieve a dynamic balance between diversification and intensification by leveraging the complementary strengths of each component, thereby enhancing the efficiency and robustness of the hybrid algorithm.

Both operators act on the same population in every iteration: dBA proposes a stochastic displacement, and WDM then moves each agent along a weighted directional vector. We make no claim about the order in which they are applied. The ablation reported in Section 5.2 finds no measurable effect of that order and shows that the benefit disappears when the coupling is delayed to the second half of the run.

Both phases are integrated sequentially and complementarily within each iteration, as follows:

(a) The dBA phase (global exploration) is executed.
(b) Subsequently, the WDM phase (local exploitation) is applied.

At each iteration, the best solution found is dynamically updated and recorded to construct the convergence curve. This hybrid structure enables the combination of the global diversification capability of dBA with the local intensification provided by WDM.

The proposed WDM-dBA scheme offers several advantages, including improved convergence stability, a reduced likelihood of being trapped in local minima, and an adaptive balance between exploration and exploitation throughout the optimization process. Additionally, it enhances the quality of the final solution, particularly in nonlinear control and optimization problems.

Table 1 presents the pseudocode of the WDM-dBA hybrid algorithm, detailing the sequence of operations that define both phases of the proposed approach. The WDM-dBA flowchart is presented in **Figure 1**.

5. Optimization of benchmark functions and the van de vusse reactor

5.1. Optimization of benchmark functions

To evaluate the optimizers on a standardized testbed with strong baselines, the five methods were assessed on the single-objective CEC 2014 benchmark suite (functions F_1–F_{30}, search domain $[-100, 100]^d$) at three dimensionalities, $d = 10, 30, 50$. The methods comprise WDM, dBA, the hybrid WDM-dBA, and two widely used population-based baselines, Particle Swarm Optimization (PSO) and Differential Evolution (DE).

All methods used the same population size (30 individuals) and the same fixed evaluation budget ($1000\,d$ function evaluations) at each dimension, so the comparison is performed on equal computational effort. Each (function, dimension) case was solved with 100 independent runs; within every run the five algorithms started from a common initial population generated with a shared seed, yielding a paired (blocked) design. The statistical analysis was pre-specified: for each function we applied a paired Wilcoxon signed-rank test of WDM against every competitor, reporting the rank-biserial effect size and p-values corrected

across the suite with Holm's procedure; a Friedman omnibus test with average ranks summarized the overall ordering. The study was implemented in Python using the opfunu 1.0.1 implementation of the suite; the code and the per-run results are deposited as described in the Code and data availability section. The per-method settings are summarized in **Table 2**.

Figures 2–4 show the median error to the known optimum, with an interquartile band, against the number of function evaluations for each function and dimension. **Table 3** reports the Friedman average ranks, and **Table 4** the per-function win/tie/loss record of WDM against each competitor at the Holm-corrected 0.05 level. Where a difference is significant, the effect is large: the median rank-biserial $|r|$ exceeds 0.88 in every pairwise comparison (overall interquartile range 0.91–1.00), so the better method prevails on almost all of the 100 paired runs of each function.

Three patterns hold consistently across the three dimensions. First, WDM clearly dominates dBA: it wins on 16, 23 and 27 functions at $d = 10, 30, 50$ while losing on at most five, confirming that the weighted-distance displacement is a substantially stronger search rule than the directional bat update. Second, WDM on its own does not match the strong baselines: against PSO, DE and the hybrid it loses on roughly 23–27 of the functions, and the Friedman test ranks it fourth of five at every dimension ($p < 10^{-12}$ in all cases). Third, and most relevant for this work, the hybrid WDM-dBA closes that gap: it ranks third overall, above either parent algorithm; a paired Wilcoxon test with Holm correction does not separate the hybrid from PSO at any dimension ($p = 0.51$–0.74), while differential evolution remains better ($p = 0.0018$–0.0139). The coupling therefore improves on both components without reaching the strongest baseline. Accordingly, the hybrid, rather than WDM in isolation, is the configuration carried forward to the NMPC control-tuning case study presented next.

Table 1. Hybridization of the WDM and dBA algorithms

Pseudocode for the hybrid WDM-dBA algorithm

Input: Parameters $N_p, N_c, my, ny, k, Ts, u, r, x_{\text{control}}, x0_{\text{plant}}$, bounds L_b, U_b, population size n, and maximum iterations $t_{\max}$
Output: Optimal matrices Q_{opt} and W_{opt}

Compute $len_Q = my \times N_p$, $len_W = \sum(N_c)$, $d = len_Q + len_W$
Initialize population $x_i \in [Lb, Ub]$, $i = 1, \ldots, n$
Evaluate $Fitness(i) = wrapper_QW_optimization(x_i, Par)$
Set $best = \arg\min(Fitness)$, $f_{min} = \min(Fitness)$
Initialize $r = r_0$, $A = A_0$, $w = (Ub - Lb)/4$
For $t = 2$ to $t_{\max}$ **do**
Phase dBA (Global Exploration)
For each individual i:
If $rand < r_i$ then $xt_i = x_i + mean(A)\,\varepsilon\, w_i$
else select $k \neq i$, compute $f_1, f_2 \in [f_{min}, f_{max}]$
$xt_i = x_i + (best - x_i)f_1 + (x_k - x_i)f_2$
Limit xt_i within $[Lb, Ub]$
Compute $F_{new} = wrapper_QW_optimization(xt_i, Par)$
If $(rand < A_i)$ and $(F_{new} < Fitness(i))$ then update $x_i = xt_i$, $Fitness(i) = F_{new}$
Phase WDM (Local Exploitation)
For each individual i:
Compute the step scale d_m, the population-mean ℓ_1 distance to the incumbent (**Equation (5)**)
Generate $P \in [Lb, Ub]$, unit vector $u_{vec} = \frac{P - x_i}{\|P - x_i\|}$
Compute weights w_g normalized by their largest component
$xt_i = x_i + w_g \cdot dist \cdot u_{vec}$
Limit xt_i within $[Lb, Ub]$
Compute $F_{new} = wrapper_QW_optimization(xt_i, Par)$
If $F_{new} < Fitness(i)$ then update $x_i = xt_i$, $Fitness(i) = F_{new}$
If $F_{new} < f_{min}$ then $best = xt_i$, $f_{min} = F_{new}$
Store $Conv_f(t) = f_{min}$
End For
Construct $Q_{opt} = diag(best(1 : len_Q))$, $W_{opt} = diag(best(len_Q + 1 : end))$
Return (Q_{opt}, W_{opt})

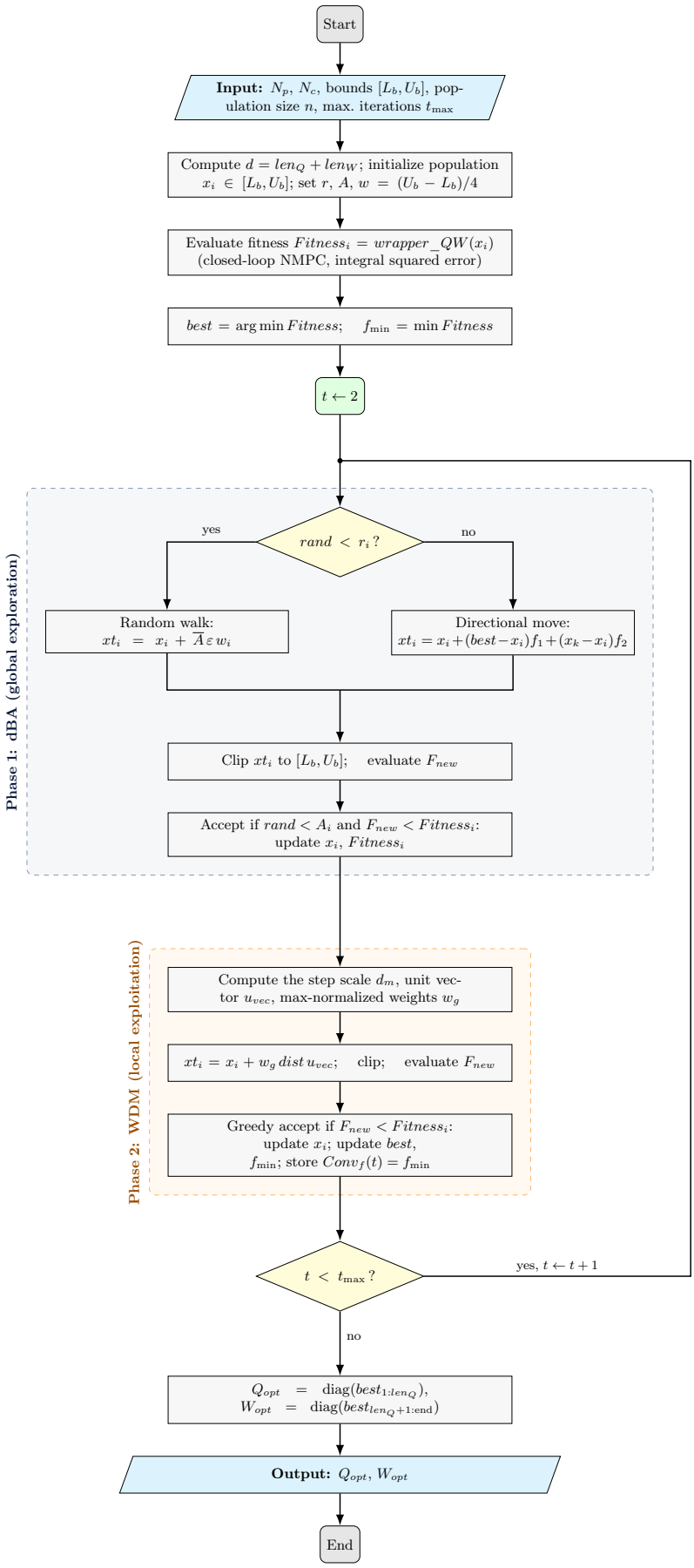


Figure 1. Flowchart of the proposed hybrid WDM-dBA algorithm for tuning the NMPC weighting matrices **Q** and **W**. Each generation applies a dBA global-exploration step (Phase 1) followed by a WDM local-exploitation step (Phase 2) for every individual, until $t_{\max}$ is reached

Table 2. Algorithm settings used in the CEC 2014 comparison. All methods share a population of 30 individuals, 100 independent runs, and a fixed budget of $1000\,d$ function evaluations. The dBA parameters follow standard literature defaults.

Method	**Settings**
WDM	Parameter-free adaptive (max-normalized) distance weights
dBA	$A_0 = 1.0$, $r_0 = 0.1$, $\alpha = 0.9$, $\gamma = 0.9$, $f \in [0, 1]$
Hybrid WDM-dBA	dBA phase (as above) followed by the WDM phase each generation
PSO	$w = 0.7298$, $c_1 = c_2 = 1.49618$, $v_{\max} = 0.2\,(\mathrm{ub} - \mathrm{lb})$
DE	rand/1/bin, $F = 0.5$, CR $= 0.9$

Table 3. Friedman average ranks (lower is better; 1 = best) of the five optimizers on the CEC 2014 suite at $d = 10, 30, 50$. The omnibus test rejects equality of ranks in every case

Method	$\boldsymbol{d = 10}$	$\boldsymbol{d = 30}$	$\boldsymbol{d = 50}$
DE	1.87	1.77	1.93
PSO	2.33	2.13	2.23
Hybrid WDM-dBA	2.37	2.57	2.50
WDM	3.87	3.80	3.57
dBA	4.57	4.73	4.77
Friedman p	4.1×10^{-13}	4.7×10^{-15}	2.6×10^{-13}

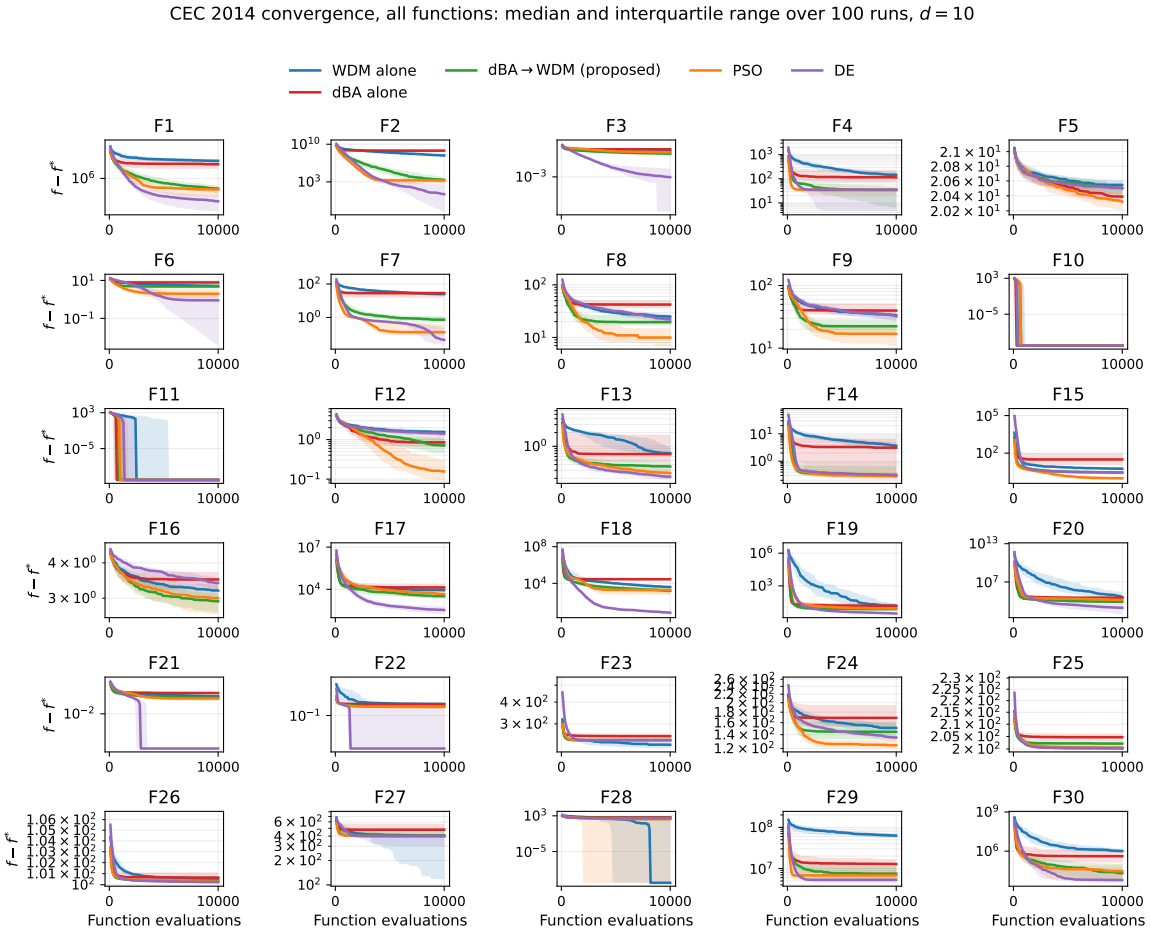


Figure 2. Convergence on the CEC 2014 suite at $d = 10$: median error to the known optimum versus the number of function evaluations (FEs), with the shaded band giving the interquartile range over 100 independent runs, for WDM, dBA, the hybrid WDM-dBA, PSO and DE. Each panel corresponds to one benchmark function F_1–F_{30}; the vertical axis uses a logarithmic scale

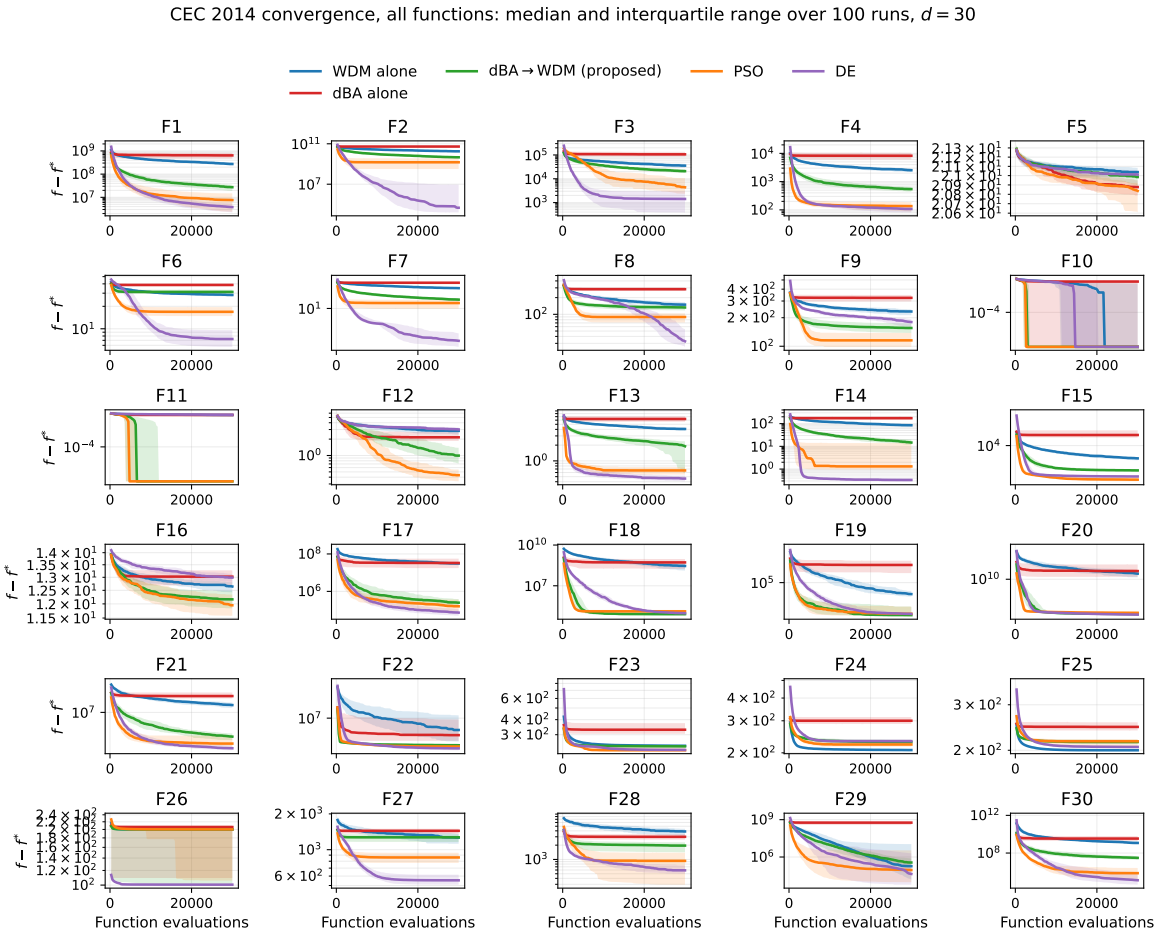


Figure 3. Convergence on the CEC 2014 suite at $d = 30$: median error to the known optimum versus the number of function evaluations (FEs), with the shaded band giving the interquartile range over 100 independent runs, for WDM, dBA, the hybrid WDM-dBA, PSO and DE. Each panel corresponds to one benchmark function F_1–F_{30}; the vertical axis uses a logarithmic scale

Table 4. Per-function comparison of WDM and the hybrid against each competitor on the CEC 2014 suite, reported as wins/ties/losses for the first method of each pair at the Holm-corrected 0.05 significance level (paired Wilcoxon signed-rank test, 100 runs per function). Totals are over the 30 functions of the suite.

Comparison	$\boldsymbol{d = 10}$	$\boldsymbol{d = 30}$	$\boldsymbol{d = 50}$
WDM vs. dBA	16/9/5	23/4/3	27/0/3
WDM vs. Hybrid	4/2/24	3/2/25	4/1/25
WDM vs. PSO	3/2/25	2/1/27	3/1/26
WDM vs. DE	3/4/23	5/0/25	7/0/23
Hybrid vs. dBA	28/1/1	29/0/1	30/0/0
Hybrid vs. WDM	24/2/4	25/2/3	25/1/4
Hybrid vs. PSO	2/16/12	3/5/22	4/4/22
Hybrid vs. DE	4/6/20	4/6/20	7/4/19

5.2. Ablation of the hybrid coupling

The submitted manuscript described the dBA→WDM ordering as principled but reported no experiment supporting it. We therefore ran an ablation that separates two questions: whether the order of the two operators matters, and whether coupling them at every iteration matters.

Eight arms were compared on the CEC 2014 suite (F_1–F_{30}) at $d = 10, 30, 50$, with 100 independent runs per case, a population of 30 and a fixed budget of $1000\,d$ evaluations for every arm. Runs share seeds across arms, so the design is paired. Five arms vary the coupling: dBA→WDM (the proposed scheme), WDM→dBA (reverse), alternating, dBA alone over the first half of the budget

followed by the coupled scheme, and each component alone. The remaining two are the PSO and DE baselines. Budget-matched versions of each component are already covered by the standalone arms, because the protocol assigns the same evaluations to every arm. The budget is enforced on evaluations rather than on generations, so a coupled generation that costs two evaluations per individual buys fewer generations and not more effort; we confirmed this by counting calls to the objective function.

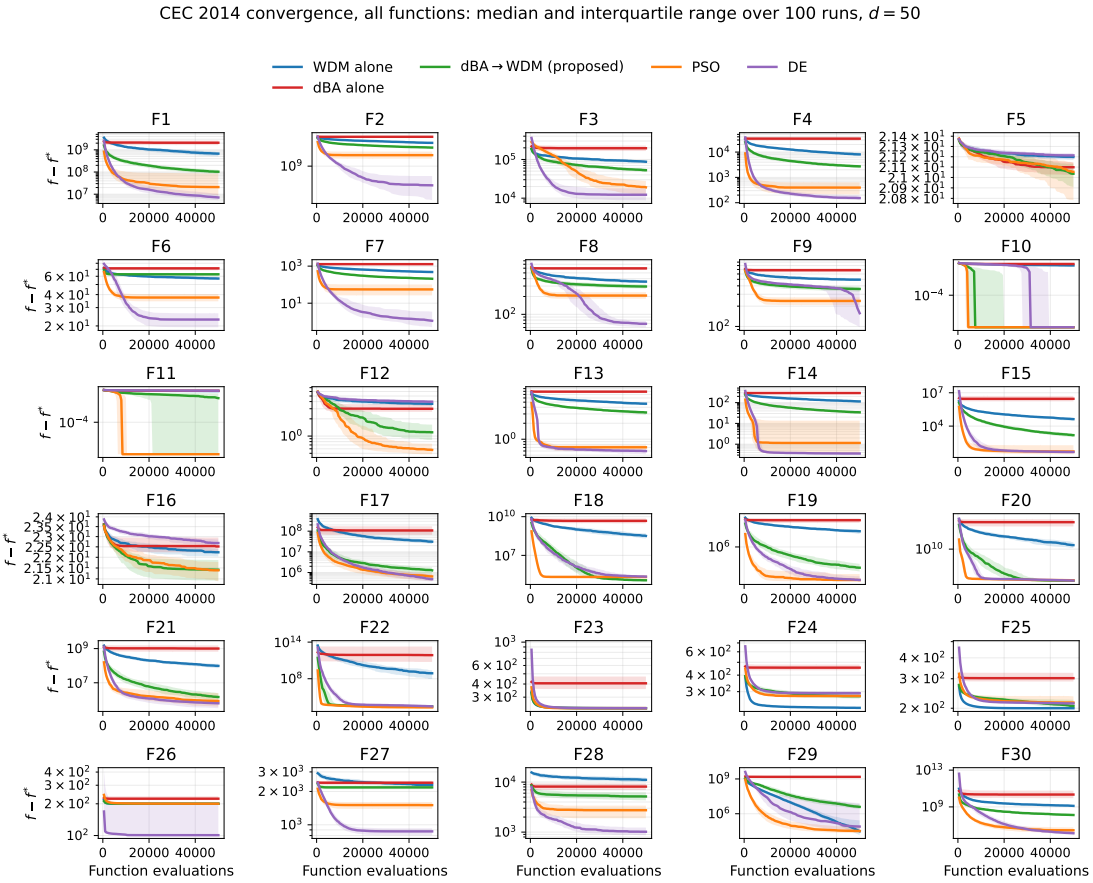


Figure 4. Convergence on the CEC 2014 suite at $d = 50$: median error to the known optimum versus the number of function evaluations (FEs), with the shaded band giving the interquartile range over 100 independent runs, for WDM, dBA, the hybrid WDM-dBA, PSO and DE. Each panel corresponds to one benchmark function F_1–F_{30}; the vertical axis uses a logarithmic scale

Table 5 reports the Friedman average ranks and **Table 6** the paired contrasts against the proposed coupling. The two blocks answer the two questions differently. The order of the operators has no measurable effect: the proposed and reverse schemes are indistinguishable at every dimension, and the alternating variant ranks marginally ahead of both without reaching significance. The per-iteration coupling, in contrast, is what the evidence supports: the proposed arm beats each component alone on 26 or more of the 30 functions at every dimension, with large effect sizes, and the arm that delays the coupling to the second half of the budget falls back to the rank of WDM alone. We therefore withdraw the claim that the ordering is principled, and state the contribution as the coupling itself.

5.3. Case study: Van de vusse reactor

To rigorously assess the effectiveness of the proposed WDM-dBA hybrid optimization framework in a realistic nonlinear control scenario, the Van de Vusse reactor is selected as a benchmark case study. This system has been extensively used in the literature as a standard testbed for advanced control strategies due to its highly nonlinear dynamics, input multiplicity, and strong coupling between mass and energy balances.[2,42] The Van de Vusse reactor represents a continuous stirred tank reactor (CSTR) in which a set of series-parallel reactions takes place, leading to the formation of both desired and undesired products.

Table 5. Friedman average ranks of the eight ablation arms (1 = best). The omnibus test rejects at every dimension: $\chi^2 = 116.58$, 123.34 and 121.99, all with $p < 10^{-21}$.

Arm	$d = 10$	$d = 30$	$d = 50$	**Mean**
DE	2.47	2.50	2.67	2.54
PSO	3.47	2.77	2.97	3.07
Alternating	3.27	3.50	3.27	3.34
WDM → dBA (reverse)	3.33	3.57	3.87	3.59
dBA → WDM (proposed)	3.67	3.77	3.40	3.61
WDM alone	6.13	6.13	5.73	6.00
dBA first half, both after	6.13	6.10	6.33	6.19
dBA alone	7.53	7.67	7.77	7.66

Table 6. Paired Wilcoxon contrasts of the proposed coupling against the other arms, across the three dimensions. Wins and losses count functions out of 30; r is the rank-biserial effect size, positive when the proposed arm is better. Holm correction applied within each dimension.

Proposed vs.	**Wins**	**Losses**	p	p_{Holm}	r	
Reverse order	13–18	12–17	0.31–0.52	0.62–0.74	−0.16	to
					+0.22	
Alternating	9–16	14–21	0.03–0.75	0.09–0.75	−0.45	to
					+0.07	
dBA first half, both after	28–29	1–2	$< 10^{-4}$	$< 10^{-4}$	+0.98	to
					+1.00	
WDM alone	26–27	3–4	$< 10^{-4}$	≤ 0.0002	+0.81	to
					+0.89	
dBA alone	29–30	0–1	$< 10^{-4}$	$< 10^{-4}$	+0.996	to
					+1.000	

The chemical reaction scheme corresponding to the Van de Vusse system is described by the following set of reactions:

$$A \xrightarrow{k_1} B$$

$$B \xrightarrow{k_2} C$$

$$2A \xrightarrow{k_3} D$$

These reactions involve the consumption of reactant A, leading to the formation of the desired product B and the undesired byproducts C and D.[9]

The reaction rate constants k_i, for $i = 1, 2$ and 3 are temperature dependent T and follow the Arrhenius law:

$$k_i(T) = k_{i0} \exp\left(-\frac{E_i}{R\,(T + 273.15)}\right), \qquad (18)$$

where E_i denotes the activation energy of each reaction and R is the universal gas constant.

The dynamic behavior of the reactor is described by the mass and energy balance equations:

$$\begin{aligned}
\frac{dC_A}{dt} &= \frac{F}{V}(C_{Af} - C_A) - k_1(T)C_A - k_3(T)C_A^2, \\
\frac{dC_B}{dt} &= -\frac{F}{V}C_B + k_1(T)C_A - k_2(T)C_B, \\
\frac{dT}{dt} &= \frac{1}{\rho C_p}\Big[k_1(T)C_A(-\Delta H_{RAB}) + k_2(T)C_B \\
&\quad \cdot(-\Delta H_{RBC}) + k_3(T)C_A^2(-\Delta H_{RAD})\Big] \\
&\quad + \frac{F}{V}(T_0 - T) + \frac{K_w A_R}{\rho C_p V}(T_k - T). \qquad (19)
\end{aligned}$$

In these equations, C_A and C_B denote the concentrations of species A and B within the reactor, respectively, while C_{Af} represents the inlet concentration. The parameter V corresponds to the reactor volume and F to the volumetric flow rate. The reactor temperature is denoted by T, with T_0 and T_k representing the inlet and jacket temperatures, respectively. Additionally, ρ is the fluid density, C_p is the specific heat capacity, K_w is the overall heat transfer coefficient, and A_R is the heat transfer area. The terms $(-\Delta H_{RAB})$, $(-\Delta H_{RBC})$ and $(-\Delta H_{RAD})$ correspond to the reaction enthalpies.

The controlled output variables are defined as $y_1 = C_B$ and $y_2 = T$, whereas the manipulated variables are $u_1 = F/V$ (dilution rate) and $u_2 = T_k$ (jacket temperature). The sampling time is $T_s = 0.05$ h, control horizon is $N_c = 14$, and the prediction horizon is $N_p = 16$, resulting in a prediction window of 0.8 h.

Operational constraints are imposed on the manipulated variables, given by $0.1\ \mathrm{h}^{-1} \leq u_1 \leq 140\ \mathrm{h}^{-1}$ and $90\ ^\circ\mathrm{C} \leq u_2 \leq 200\ ^\circ\mathrm{C}$. The model parameters in **Equation (19)** were adopted from.[9]

5.3.1. Results and discussions

This section presents the results obtained using the hybrid WDM-dBA algorithm for the optimization of the weighting parameters associated with performance and control effort in a Van de Vusse reactor.

The control of this system is particularly challenging due to the presence of parallel and consecutive reactions, which introduce intrinsic nonlinearities and competing pathways, making the maximization of the desired product concentration a nontrivial objective. In addition, the strong temperature dependence of the reaction kinetics, typically described by Arrhenius-type expressions, leads to highly sensitive and nonlinear system dynamics.

The dynamic model of the reactor, described by the coupled mass and energy balance equations in **Equation (19)**, exhibits characteristics such as multiple steady states, strong input/output interactions, and sensitivity to disturbances. These features make the reactor particularly suitable for evaluating NMPC strategies, as conventional linear control approaches are generally insufficient to guarantee satisfactory performance. Within the NMPC framework, the control problem is formulated as a constrained nonlinear optimization problem that is solved at each sampling instant. The objective function penalizes both the tracking error and the control effort, requiring an appropriate balance between performance and actuator usage.[4] However, the selection of the weighting matrices in the cost function remains a challenging task, as it directly influences closed-loop stability, transient response, and robustness against disturbances. From an optimization perspective, the tuning of NMPC parameters constitutes a high-dimensional, nonlinear, and nonconvex problem. The interaction between process nonlinearities and control constraints often leads to complex optimization landscapes with multiple local minima, where traditional tuning methods or gradient-based approaches may fail to identify globally optimal solutions. In this context, metaheuristic optimization methods provide a suitable alternative due to their ability to perform global search in complex spaces.[20] In this work, the proposed WDM-dBA hybrid algorithm is employed to optimize the weighting matrices of the NMPC controller. The hybrid structure enables a coordinated search process in which the global exploration capability of the directional bat algorithm identifies promising regions of the search space, while the weighted distance mechanism exploits local structural information to refine candidate solutions. This interaction is particularly advantageous in the Van de Vusse reactor, where the nonlinear coupling between variables requires both global exploration and precise local adjustments to achieve optimal control performance. The evaluation is carried out through servo control tests involving setpoint changes in both the concentration of the desired product and the reactor temperature. The dynamic response of the system under different MPC tuning schemes is illustrated in **Figures 5–9**. The reference trajectory for the concentration output y_1 is modified from 0.9052 mol/L to 1.0 mol/L at $t = 0.3$ h. For the temperature output y_2, the reference value is changed from 134.95 °C to 130 °C at $t = 3.9$ h, and subsequently to 120 °C at $t = 5.3$ h. The results (**Figures 5–9**) show that the proposed hybrid approach produces smooth control actions and accurate setpoint tracking, achieving closed-loop performance comparable to the standalone optimization methods on this case study (**Tables 7** and **8**). To further assess the algorithm's sensitivity to parameter configuration and its stochastic repeatability, **Table 8** presents the statistical distribution of the hybrid WDM-dBA algorithm across eight independent runs for population sizes of $n = 10$ and $n = 20$. The results indicate that both population sizes maintain extremely low median errors for concentration C_B and temperature T, on the order of 10^{-7} or lower, demonstrating high consistency across random initializations. Although increasing the population size from $n = 10$ to $n = 20$ slightly increases the computational execution time from 14:32 to 17:15 minutes, the variance and standard deviation remain virtually unchanged. This confirms that a smaller population of $n = 10$ agents is sufficient to ensure robust convergence without incurring an unnecessary computational burden. Additionally, the optimized controller maintains the manipulated variables within operational constraints, indicating an effective balance between performance and control effort. These results confirm that the integration of the WDM-dBA algorithm within

the NMPC framework provides a robust and efficient strategy for handling complex nonlinear control problems, particularly in systems characterized by strong coupling and high sensitivity such as the Van de Vusse reactor.

The integral of the squared error (ISE) is employed as a performance index to evaluate the controllers, as it accounts for both transient behavior, including overshoot, and settling characteristics. In the discrete-time domain, the ISE is defined as:

$$\text{ISE} = \sum_{k=1}^{N} (r_k - y_k)^2,$$

where r_k denotes the reference signal, y_k represents the system output at the k-th sampling instant, and N is the total number of samples.
In addition, the control performance is further assessed using the root-mean-square error (RMSE), defined as:

$$\text{RMSE} = \sqrt{\frac{ISE}{N}} \times 100.$$

To quantitatively evaluate control performance, the ISE and RMSE were computed for the controlled variables; see **Table 7**. The hybrid WDM-dBA algorithm achieved lower values compared with standalone methods, confirming improved tracking performance and reduced oscillatory behavior.

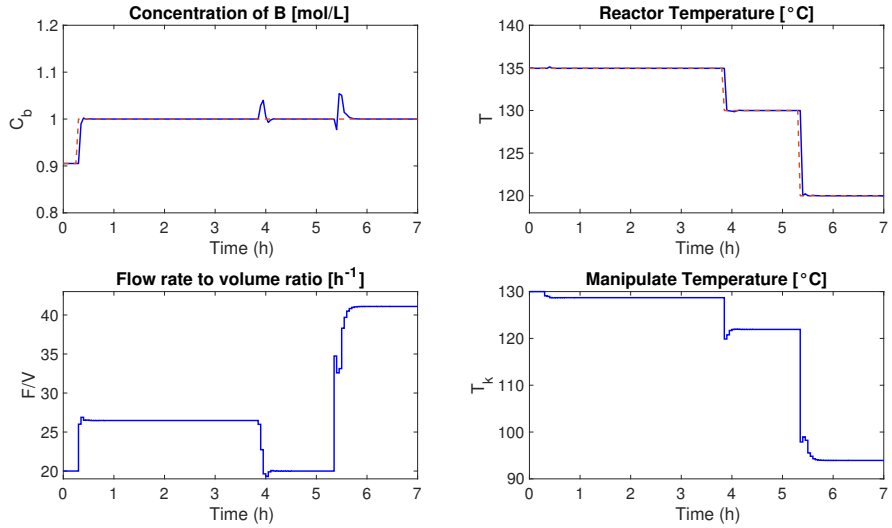


Figure 5. Servo control test for the Van de Vusse reactor case study. Optimized penalty parameters obtained using dBA, $Q_{11} = 2.2569$, $Q_{22} = 2.7784$, $W_{11} = 1.0 \times 10^{-4}$, $W_{22} = 1.0 \times 10^{-4}$

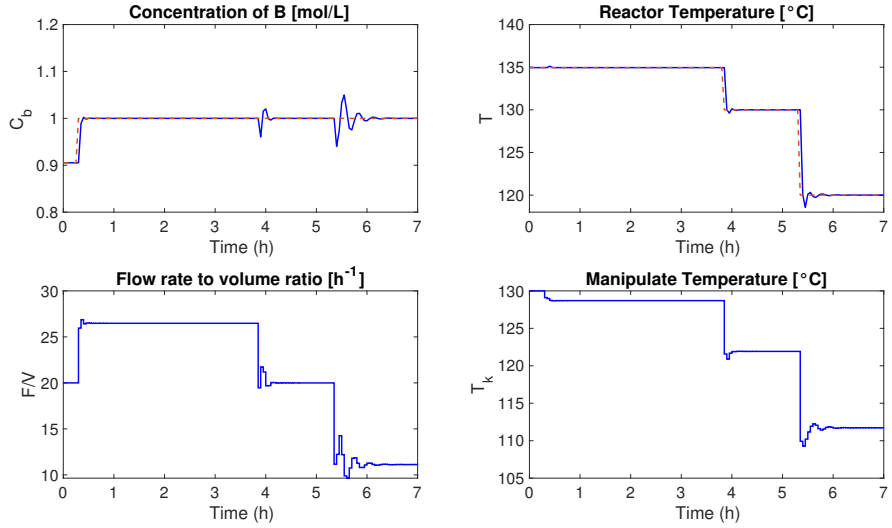


Figure 6. Servo control test for the Van de Vusse reactor case study. Optimized penalty parameters obtained using WDM, $Q_{11} = 5.1341$, $Q_{22} = 5.2819$, $W_{11} = 0.0001$, $W_{22} = 0.0054$

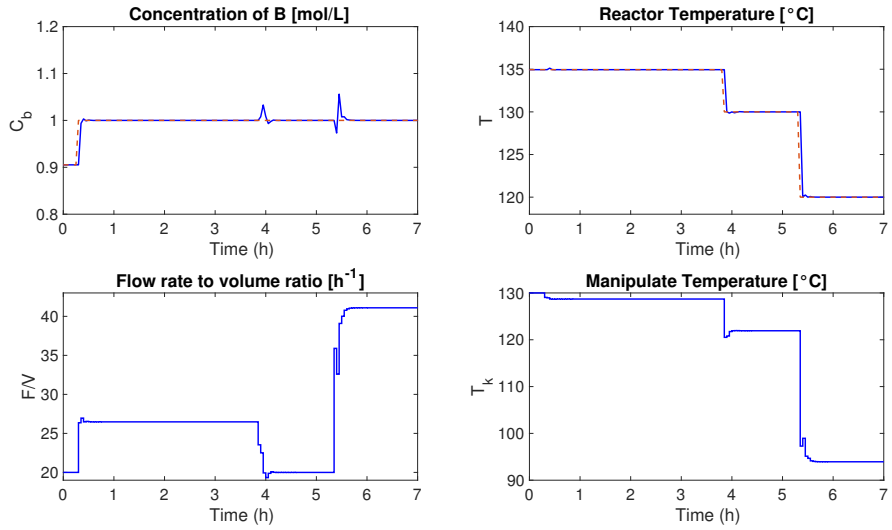


Figure 7. Servo control test for the Van de Vusse reactor case study. Optimized penalty parameters obtained using the hybrid WDM-dBA algorithm, $Q_{11} = 8.4257$, $Q_{22} = 4.2135$, $W_{11} = 1.0 \times 10^{-4}$, $W_{22} = 1.0 \times 10^{-4}$

Table 7. Comparative performance analysis of the hybrid WDM-dBA, WDM, and dBA algorithms based on the ISE and RMSE metrics, where RMSE $= 100\sqrt{\text{ISE}/N}$ and N is the number of samples in the error sequence ($N = 150$ for the reported values). Time is reported as mm:ss.

C_b	**Hybrid WDM-dBA**	**WDM**	**dBA**
ISE	0.0142	0.0208	0.0179
RMSE	0.9756	1.1792	1.0933
T	**Hybrid WDM-dBA**	**WDM**	**dBA**
ISE	124.6461	127.0154	124.6311
RMSE	91.1577	92.0200	91.1522
Time	00:00:16	00:00:22	00:00:18

Table 8. Comparative performance of the WDM-dBA hybrid algorithm for population sizes of $n = 10$ and $n = 20$ agents over eight independent runs

C_b	$n = 10$	$n = 20$
Mean error	-4.0554×10^{5}	-5.9118×10^{-5}
Median error	-2.9300×10^{-7}	-2.3291×10^{-7}
Variance	1.1111×10^{-4}	9.9497×10^{-5}
Standard deviation	1.0541×10^{-2}	9.9748×10^{-3}
T	$n = 10$	$n = 20$
Mean error	-1.1309×10^{-1}	-1.4416×10^{-1}
Median error	-9.1758×10^{-8}	5.6843×10^{-14}
Variance	8.8397×10^{-1}	9.9210×10^{-1}
Standard deviation	9.4020×10^{-1}	9.9604×10^{-1}
Mean ISE	131.7294	148.7838
Median ISE	124.6803	124.6627
Time	00:14:32	00:17:15

The improved performance of the WDM-dBA algorithm can be attributed to the interaction between exploration and exploitation mechanisms. While dBA promotes global search diversity, WDM refines solutions using distance-based information from the population. The dispersion across runs does not support a claim of smoother convergence in terms of final error distribution: the interquartile width of the final error, normalized by the median, is 0.871 for the hybrid at $d = 10$ against 0.412 for WDM and 0.312 for DE. Nevertheless, this broader dispersion reflects a more exploratory search behavior rather than algorithmic failure; the hybrid consistently avoids poor local traps across all stochastic seeds, ensuring that initialization robustness is preserved even if the final objective spread is wider. The coupling also does not increase the computational cost, because the budget is fixed in function evaluations: at $d = 50$ the hybrid averages 22.1 s per run against 22.4 s for WDM and 22.0 s for dBA.

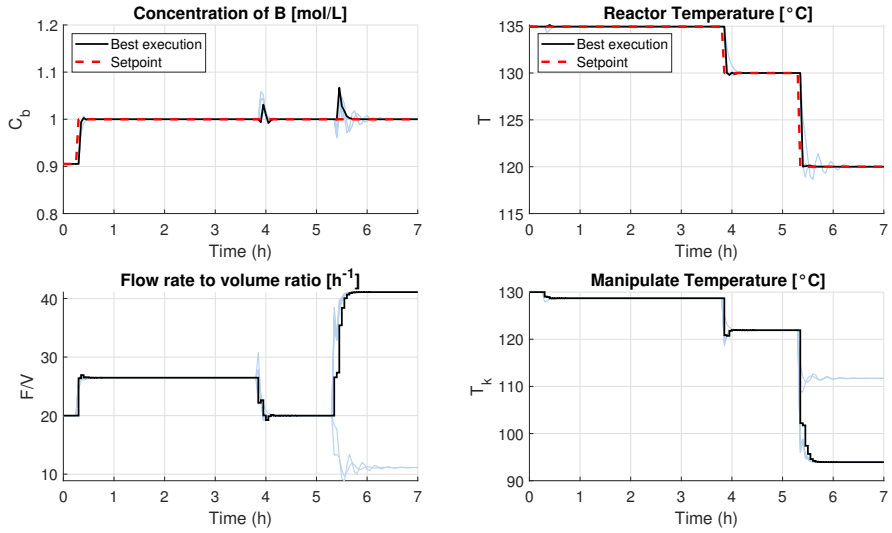


Figure 8. Servo control test for the Van de Vusse reactor case study using 10 randomly initialized agents over eight independent runs. The black line represents the best-performing run, with $Q_{11} = 10$, $Q_{22} = 0.3812$, $W_{11} = 1.0 \times 10^{-4}$, and $W_{22} = 1.0 \times 10^{-4}$

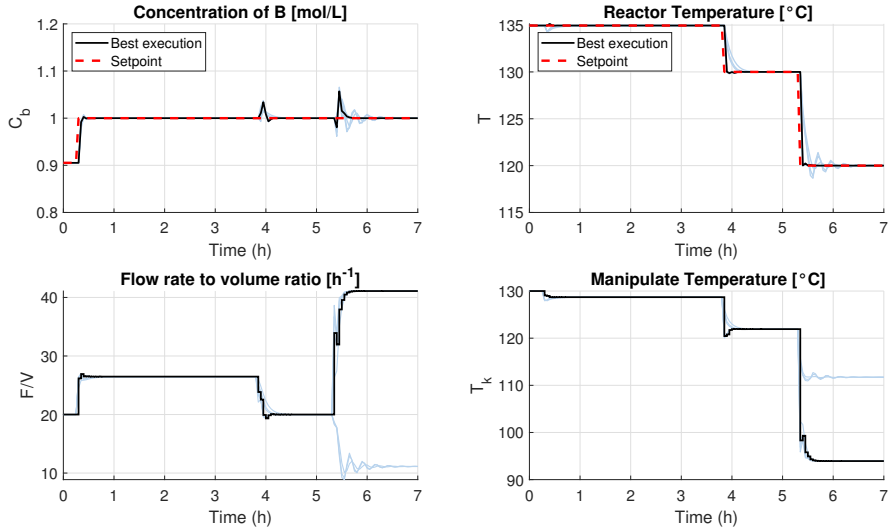


Figure 9. Servo control test for the Van de Vusse reactor case study using 20 randomly initialized agents over eight independent runs. The black line represents the best-performing run, with $Q_{11} = 4.4168$, $Q_{22} = 2.2955$, $W_{11} = 1.0 \times 10^{-4}$, and $W_{22} = 1.0 \times 10^{-4}$

6. Conclusion

This work presented a hybrid optimization framework that combines WDM with dBA for parameter tuning in NMPC applications. The proposed approach was specifically designed to address common limitations of metaheuristic algorithms, particularly the imbalance between exploration and exploitation and the loss of convergence stability in high-dimensional optimization problems. The CEC 2014 study, conducted at $d = 10, 30, 50$ against PSO and DE baselines with a pre-specified statistical protocol, shows that WDM substantially outperforms the standalone dBA (winning on 16–27 of the functions across dimensions), confirming that the distance-based adaptive mechanism is a stronger search rule than the directional bat update. WDM in isolation, however, does not match the strong baselines and ranks fourth of five under the Friedman test. The hybrid WDM-dBA closes this gap: it ranks third overall, above either parent algorithm, statistically indistinguishable from PSO (Holm-corrected $p = 0.51$–0.74) and below DE, which indicates that the contribution of this work lies in the coupling of dBA's exploration with WDM's exploitation rather than in WDM alone. When applied to the NMPC tuning problem of the Van de Vusse reactor, the hybrid WDM-dBA algorithm achieved accurate tracking of both concentration and temperature setpoints while maintaining smooth and bounded control actions.Although its overall closed-loop performance was comparable to that of the independent methods in temperature tracking (**Tables 7** and **8**), the hybrid scheme achieved improved tracking accuracy in concentration alongside enhanced convergence stability and robustness to initialization. From a control perspective, the results highlight the importance of properly tuning the weighting matrices in NMPC formulations, particularly in systems characterized by strong nonlinearities and variable coupling such as the Van de Vusse reactor. The proposed optimization strategy proved capable of handling the resulting non-convex search space, providing parameter configurations that enhance both robustness and dynamic performance. Furthermore, the integration of a distance-based weighting mechanism within a hybrid metaheuristic framework introduces a structured way of exploiting population information, which contributes to improved convergence behavior without sacrificing exploration capabilities. This feature is especially relevant for large-scale or high-dimensional optimization problems commonly encountered in process systems engineering. Overall, the proposed WDM-dBA framework represents a robust and efficient alternative for solving complex optimization problems in NMPC, with potential applications extending beyond chemical reactors to other nonlinear and constrained systems. Several limitations bound the scope of these findings. The control study validated the method on a single process, the Van de Vusse reactor (a two-input, two-output system), so its advantage on larger or differently structured plants remains to be established. The weighting matrices Q and W were assumed diagonal, which shrinks the tuning space but cannot represent cross-channel penalties. In the closed-loop task, all three metaheuristics achieved competitive tracking performance (**Tables 7** and **8**); however, the practical advantage of the hybrid approach lies in its enhanced convergence stability, robustness to initialization, and improved tracking performance in key states. Finally, on the CEC 2014 suite the hybrid does not surpass the DE and PSO baselines; its role is to close the gap left by WDM and dBA individually rather than to define a new benchmark standard. These boundaries should be weighed when transferring the approach to higher-dimensional or real-time NMPC problems.

Future work will focus on extending the proposed approach to multi-objective optimization frameworks, incorporating uncertainty and disturbance handling within the NMPC scheme, and assessing its performance in real-time and industrial-scale applications. Additionally, efforts will be directed toward enhancing the computational efficiency of the algorithm to facilitate its practical implementation in complex process systems.

Acknowledgments

The authors acknowledge the support of Universidad Juárez Autónoma de Tabasco, Universidad de Guanajuato, and Universidad Autónoma de Querétaro for the development of this research.

Funding

None.

Conflict of interest

The authors declare they have no competing interests.

Author contributions

Conceptualization: Misael Hernández, Luis Miguel Valenzuela, Antioco López-Molina, Fernando Israel Gómez-Castro
Formal analysis: Luis Miguel Valenzuela, Fernando Israel Gómez-Castro, Oscar Daniel Lara-Montaño
Investigation: Luis Miguel Valenzuela, Antioco López-Molina, Carolina Conde-Mejía, Fernando Israel Gómez-Castro, Oscar Daniel Lara- Montaño, Moisés Abraham Petriz-Prieto
Methodology: Misael Hernández, Luis Miguel Valenzuela, Antioco López-Molina, Carolina Conde-Mejía, Fernando Israel Gómez-Castro, Oscar Daniel Lara-Montaño, Moisés Abraham Petriz-Prieto
Writing–original draft: Misael Hernández, Luis Miguel Valenzuela, Antioco López-Molina, Oscar Daniel Lara-Montaño
Writing-review & editing: Luis Miguel Valenzuela, Antioco López-Molina, Fernando Israel Gómez-Castro, Oscar Daniel Lara-Montaño

Availability of data

The optimizer implementations, the experiment driver, the analysis scripts and the per-run results of the benchmark study are deposited in a public repository, together with the pinned software environment and the seeds needed to reproduce every table and figure. The raw closed-loop trajectories of the control case study are included in the same deposit. The digital object identifier is [https://doi.org/10.5281/zenodo.22971624].

AI tools statement

During the preparation of this work, the authors used Gemini in order to improve the English language and readability.

References

1. Qin SJ, Badgwell TA. A survey of industrial model predictive control technology. *Control Eng Pract.* 2003;11(7):733-764. https://doi.org/10.1016/S0967-0661(02)00186-7
2. Engell S. Feedback control for optimal process operation. *J Process Control.* 2007;17(3):203-219. https://doi.org/10.1016/j.jprocont.2006.10.011
3. Wang L. *Model Predictive Control System Design and Implementation Using MATLAB.* London, UK: Springer; 2009. https://doi.org/10.1007/978-1-84882-331-0
4. Rawlings JB, Mayne DQ, Diehl MM. *Model Predictive Control: Theory, Computation, and Design.* 2nd ed. Madison, WI: Nob Hill Publishing; 2017. Accessed January 9, 2026. https://sites.engineering.ucsb.edu/˜jbraw/mpc/MPC-book-2nd-edition-1st-printing.pdf
5. Patrón GD, Ricardez-Sandoval LA. A robust nonlinear model predictive controller for a post-combustion CO_2 capture absorber unit. *Fuel.* 2020;265:116932. https://doi.org/10.1016/j.fuel.2019.116932
6. Lucia S, Finkler T, Engell S. Multi-stage nonlinear model predictive control applied to a semi-batch polymerization reactor under uncertainty. *J Process Control.* 2013;23(9):1306-1319. https://doi.org/10.1016/j.jprocont.2013.08.008
7. Vallerio M, Van Impe J, Logist F. Tuning of NMPC controllers via multi-objective optimisation. *Comput Chem Eng.* 2014;61:38-50. https://doi.org/10.1016/j.compchemeng.2013.10.003
8. Flores-Tlacuahuac A, Morales P, Rivera-Toledo M. Multiobjective nonlinear model predictive control of a class of chemical reactors. *Ind Eng Chem Res.* 2012;51(17):5891-5899. https://doi.org/10.1021/ie201742e
9. Giraldo SAC, Melo PA, Secchi AR. Tuning of model predictive controllers based on hybrid optimization. *Processes.* 2022;10(2):351. https://doi.org/10.3390/pr10020351
10. Al Bannoud M, da Silva CAM, Martins TD. Applications of metaheuristic optimization algorithms in model predictive control for chemical engineering processes: A systematic review. *Annu Rev Control.* 2024;58:100973. https://doi.org/10.1016/j.arcontrol.2024.100973
11. Ölmez Y, Koca GÖ, Akpolat ZH. Recent metaheuristics on control parameter determination. *Int J Optim Control Theor Appl.* 2025;15(1):166-182. https://doi.org/10.36922/ijocta.1620
12. Joseph SB, Dada EG, Abidemi A, Oyewola DO, Khammas BM. Metaheuristic algorithms for PID controller parameters tuning: Review, approaches and open problems. *Heliyon.* 2022;8(5):e09399. https://doi.org/10.1016/j.heliyon.2022.e09399
13. Kennedy J, Eberhart R. Particle swarm optimization. In: *Proceedings of ICNN'95 - International Conference on Neural Networks.* Vol 4. Piscataway, NJ: IEEE; 1995:1942-1948. https://doi.org/10.1109/ICNN.1995.488968
14. Storn R, Price K. Differential evolution - A simple and efficient heuristic for global optimization over continuous spaces. *J Glob Optim.* 1997;11(4):341-359. https://doi.org/10.1023/A:1008202821328
15. Yang XS. A new metaheuristic bat-inspired algorithm. In: *Nature Inspired Cooperative Strategies for Optimization (NICSO 2010).* Studies in Computational Intelligence, Vol 284. Berlin, Germany: Springer; 2010:65-74. https://doi.org/10.1007/978-3-642-12538-6_6
16. Mirjalili S, Lewis A. The whale optimization algorithm. *Adv Eng Softw.* 2016;95:51-67. https://doi.org/10.1016/j.advengsoft.2016.01.008

17. Benaissa B, Kobayashi M, Al Ali M, Khatir T, Elaissaoui Elmeliani MEA. Metaheuristic optimization algorithms: An overview. *HCMCOU J Sci Adv Comput Struct.* 2024;14(1):33-61. https://doi.org/10.46223/hcmcoujs.acs.en.14.1.47.2024
18. Houssein EH, Saeed MK, Hu G, Al-Sayed MM. Metaheuristics for solving global and engineering optimization problems: Review, applications, open issues and challenges. *Arch Comput Methods Eng.* 2024;31:4485-4519. https://doi.org/10.1007/s11831-024-10168-6
19. Delgarm Z, Mostafa Gharebaghi AR, Emami A. Comparison of metaheuristic algorithms for weight optimization of a semi-submersible VAWT substructure with hexagonal pontoons. *Int J Marit Technol.* 2026;22(1):66-80. https://doi.org/10.66224/ijmt.22.1.66
20. Tomar V, Bansal M, Singh P. Metaheuristic algorithms for optimization: A brief review. In: *Engineering Proceedings (RAiSE-2023).* Vol 59. Basel, Switzerland: MDPI; 2024:238. https://doi.org/10.3390/engproc2023059238
21. Wolpert DH, Macready WG. No free lunch theorems for optimization. *IEEE Trans Evol Comput.* 1997;1(1):67-82. https://doi.org/10.1109/4235.585893
22. Kusznir T, Smoczek J. Nonlinear model predictive control with evolutionary data-driven prediction model and particle swarm optimization optimizer for an overhead crane. *Appl Sci.* 2024;14(12):5112. https://doi.org/10.3390/app14125112
23. Devanathan B, Selvaraj P, Suyampulingam A. Nonlinear model predictive control for Internet of Things using particle swarm optimization and cloud computing. *IEEE Access.* 2025;99:1. https://doi.org/10.1109/ACCESS.2025.3554719
24. Essa MESM, Elsisi M, Saleh Elsayed M, Fawzy Ahmed M, Elshafeey AM. An improvement of model predictive for aircraft longitudinal flight control based on intelligent technique. *Mathematics.* 2022;10(19):3510. https://doi.org/10.3390/math10193510
25. Liu L, Liu H, Wang X, *et al.* Application of path planning and tracking control technology in mower robots. *Agronomy.* 2024;14(11):2473. https://doi.org/10.3390/agronomy14112473
26. Ewias AM, Hakmi SH, Mohamed TH, *et al.* Advanced load frequency control of microgrid using a bat algorithm supported by a balloon effect identifier in the presence of photovoltaic power source. *PLoS One.* 2023;18(10). https://doi.org/10.1371/journal.pone.0293246
27. Zhao J, Chang G, Sun Y, *et al.* Real-time nonlinear model predictive control for optimizing the ammonia coverage ratio of an SCR system based on TC-QPSO. *Control Eng Pract.* 2023;132:105409. https://doi.org/10.1016/j.conengprac.2022.105409
28. Zhang L, Xie L, Su H, Liu J. Data-driven auto-tuning strategy for RTO-MPC based on Bayesian optimization. *Comput Chem Eng.* 2024;187:108743. https://doi.org/10.1016/j.compchemeng.2024.108743
29. Meng Z, Xiao Y, Xu X, Luo B, Du Y, Gui W. Auto-tuning strategy for deep Koopman robust model predictive control design based on advanced metaheuristics. *Neurocomputing.* 2025;638:130197. https://doi.org/10.1016/j.neucom.2025.130197
30. Ławryńczuk M. Koopman operator-based multimodel for predictive control. *Nonlinear Dyn.* 2024;116:19085-19110. https://doi.org/10.1007/s11071-024-09615-7
31. Dahak A, Boutaghane H, Boulmaiz T. Machine and deep learning-based prediction of infiltration parameters: insights from field data in Northern Algeria. *Euro-Mediterr J Environ Integr.* 2026;11(4):58. https://doi.org/10.1007/s41207-026-01103-1
32. Ankalugari S, Abuthahir MU, Jan NM, Joseph AG. Control of van de Vusse reactor using deep reinforcement learning. In: *2024 29th International Conference on Automation and Computing (ICARCV).* Piscataway, NJ: IEEE; 2024:1-6. https://doi.org/10.1109/ICARCV63323.2024.10821642
33. Wang Y, Wang P, Zhang J, *et al.* A novel bat algorithm with multiple strategies coupling for numerical optimization. *Mathematics.* 2019;7(2):135. https://doi.org/10.3390/math7020135
34. Yu H, Song J, Chen C, *et al.* Optimal performance design of bat algorithm: An adaptive multi-stage structure. *CAAI Trans Intell Technol.* 2025;10(3):755-814. https://doi.org/10.1049/cit2.12377
35. Qin F, Zain AM, Zhou KQ, *et al.* Hybrid harmony search algorithm integrating differential evolution and Lévy flight for engineering optimization. *IEEE Access.* 2025;13:13534-13572. https://doi.org/10.1109/ACCESS.2025.3529714
36. Bansal S, Bhattacharjee S. An improved quantum-inspired evolutionary algorithm framework implemented to solve minimum vertex cover problem. *Struct Multidisc Optim.* 2025;68(7):145. https://doi.org/10.1007/s00158-025-04078-9
37. Bindu MG, Malathi S. Explainable feature selection using improved firefly algorithm with population diversification and stagnation-aware exploration. *Discov Comput.* 2026;29:149. https://doi.org/10.1007/s10791-026-10041-z
38. Zhang K, Zhao H, Li X, Fu C, Jin J. Gekko japonicus algorithm: A novel nature-inspired algorithm for engineering problems and path planning. *J Bionic Eng.* 2026;23(1):431-471. https://doi.org/10.1007/s42235-025-00805-6
39. Yahaya MS, Hashim ASB, Balogun AO, *et al.* Exploration and exploitation mechanism in pairwise

test case generation: A systematic literature review. *IEEE Access*. 2025;13:82342-82377. https://doi.org/10.1109/ACCESS.2025.3566163

40. Chakri A, Khelif R, Benouaret M, Yang XS. New directional bat algorithm for continuous optimization problems. *Expert Syst Appl*. 2017;69:159-175. https://doi.org/10.1016/j.eswa.2016.10.050
41. Trierweiler JO, Engell S. Controllability analysis via the robust performance number for a CSTR with Van de Vusse reaction. In: *Proceedings of the 1997 European Control Conference (ECC)*. Piscataway, NJ: IEEE; 1997:3083-3088. https://doi.org/10.23919/ECC.1997.7082582
42. Klatt KU, Engell S. Gain-scheduling trajectory control of a continuous stirred tank reactor. *Comput Chem Eng*. 1998;22(4-5):491-502. https://doi.org/10.1016/S0098-1354(97)00261-5

Misael Hernández *received the B.Eng. degree in Petrochemical Engineering from the Autonomous Juárez University of Tabasco (UJAT), Mexico, where he is currently pursuing the M.Sc. degree in Science and Technology. His research interests include scientific programming, computational efficiency analysis of metaheuristic algorithms, the numerical stability of high-dimensional optimization methods, and the development of advanced exploitation strategies to accelerate convergence toward optimal solutions.*
https://orcid.org/0009-0000-1291-7797

Luis Miguel Valenzuela *received the B.Sc. degree in Mathematics and the M.Sc. degree in Applied Mathematics from the Autonomous Juárez University of Tabasco (UJAT), Mexico. He earned the Ph.D. degree in Mathematical Sciences from the Faculty of Sciences at the National Autonomous University of Mexico (UNAM). His research interests include optimization, control engineering, and continuous dynamical systems. He has published in international peer-reviewed journals and presented his work at numerous national and international conferences. He is actively engaged in both research and higher education teaching.*
https://orcid.org/0000-0002-9918-3032

Antioco López-Molina *received the Ph.D. degree in Chemical Engineering from the Instituto Tecnológico de Celaya, Mexico. His research interests include process safety, chemical process optimization, risk assessment, and industrial process engineering. He has participated in research projects and published scientific articles in the fields of process safety and chemical engineering. He is currently engaged in teaching and research activities related to process engineering and optimization.*
https://orcid.org/0000-0001-6486-0059

Carolina Conde-Mejía *received the Ph.D. degree in Chemical Engineering from the Instituto Tecnológico de Celaya, Mexico. She is a Professor and Researcher at the Universidad Juárez Autónoma de Tabasco. Her research interests include process design, biofuels, bioproducts, process optimization, and sustainable chemical engineering. She has published scientific articles in international journals and participates in research projects related to process engineering and biorefinery systems.*
https://orcid.org/0000-0001-8162-9094

Fernando Israel Gómez-Castro *received the Ph.D. degree in Chemical Engineering from the Instituto Tecnológico de Celaya, Mexico. He is a Full Professor in the Department of Chemical Engineering at the University of Guanajuato. His research interests include process design, process optimization, mathematical modeling, process intensification, and biorefinery systems. He has authored numerous scientific publications in these fields.*
https://orcid.org/0000-0003-4906-063X

Oscar Daniel Lara-Montaño *received the Ph.D. degree in Chemical Engineering Sciences from the University of Guanajuato, Mexico. His research interests include process optimization, process systems engineering, mathematical optimization, heat exchanger design, and metaheuristic algorithms. He has published scientific articles in international journals on process optimization and sustainable engineering.*
https://orcid.org/0000-0003-2055-1216

Moisés Abraham Petriz-Prieto *received the Ph.D. degree in Chemical Engineering Sciences from the Instituto Tecnológico de Celaya, Mexico. He is a Professor and Researcher at the Universidad Juárez Autónoma de Tabasco (UJAT), Mexico. His research interests include chemical process engineering, process optimization, and sustainable process development. He has published scientific articles in indexed journals related to chemical engineering and process systems.*
https://orcid.org/0000-0002-9800-4565

An International Journal of Optimization and Control: Theories & Applications (https://accscience.com/journal/ijocta)



This work is licensed under a Creative Commons Attribution 4.0 International License. The authors retain ownership of the copyright for their article, but they allow anyone to download, reuse, reprint, modify, distribute, and/or copy articles in IJOCTA, so long as the original authors and source are credited. To see the complete license contents, please visit http://creativecommons.org/licenses/by/4.0/.